Received 14 April 2020; accepted 20 May 2020. Date of publication 2 June 2020; date of current version 24 June 2020.
The review of this article was arranged by Editor M. Chan.

Digital Object Identifier 10.1109/JEDS.2020.2999269

Schottky Barrier Height Analysis of Diamond SPIND Using High Temperature Operation up to 873 K

M. MALAKOUTIAN [1,4] (Member, IEEE), M. BENIPAL [2], F. A. KOECK [3], R. J. NEMANICH [3], AND S. CHOWDHURY [4] (Senior Member, IEEE)

1 Electrical and Computer Engineering Department, University of California at Davis, Davis, CA 95616, USA
2 Advent Diamond Inc., Scottsdale, AZ 85287, USA
3 Department of Physics, Arizona State University, Tempe, AZ 85287, USA
4 Department of Electrical Engineering, Stanford University, Stanford, CA 94305, USA

CORRESPONDING AUTHORS: M. MALAKOUTIAN (e-mail: malakout@stanford.edu) and S. CHOWDHURY

This work was supported by National Aeronautics and Space Administration (NASA) through as part of the HOTTech Program under Grant NNX17AG45G.

ABSTRACT In this work, the high temperature performance of a diamond Schottky PIN diode is reported in the range of 298-873 K. The diamond diode exhibited an explicit rectification up to 723 K with an excellent forward current density of >3000 A/cm^2. The stability of the diode was investigated by exposing the sample to high temperature cycles (up to 873 K) for more than 10 times (totaling up to 120 hours), which exhibited no change between the I-V characteristics measured in each cycle. The dependence of ideality factor and Schottky barrier height on temperature along with an extracted Richardson's constant much smaller than the theoretical value (0.0461 A/cm^2.K^2), motivated us to study the possible reason for this anomaly. A modified thermionic emission model following Tung's analysis was used to explain the experimental observations. The model assumed the presence of inhomogeneous Schottky barrier heights leading to a reduced effective area and yielded a Richardson's constant closer to the theoretical value. Conductive atomic force microscopy studies were conducted, which concurred with the electrical data and confirmed the presence of inhomogeneous Schottky barrier heights.

INDEX TERMS Diamond, Schottky PIN diode (SPIND), high temperature operation, barrier height.

I. INTRODUCTION

Diamond as a wide bandgap (∼5.45 eV) material with outstanding thermal properties is attractive for power electronics. Since diamond has deep level p- and n-type dopants (boron is 0.37 eV above the valence band and phosphorus is 0.57 eV below the conduction band), high temperature environment increases the number of activated dopants. As a result, diamond semiconductor devices show a superior operation at high temperatures. Besides conventional Schottky barrier diodes [1]–[4], Schottky PN and PIN diodes (SPND/SPIND) [5]–[10] are well-known in diamond, where the n-type and intrinsic layers are depleted by a highly boron doped (p+) layer. This makes SPNDs/SPINDs unipolar devices where the current is due to the thermionic emission (TE) of holes [6]. The electrical characteristics of the Schottky diode is determined by the Schottky barrier property and can depend on the surface preparation during the fabrication process. An imperfect surface/interface could cause inhomogeneity leading to non-ideal diode behavior in diamond similar to Si, GaN, and SiC [11]–[15]. This non-ideality includes measurement of different ideality factors (n) and Schottky barrier heights (SBHs) at different temperatures and also extraction of a much smaller effective Richardson's constant (A^{**}) using conventional TE model. Non-ideal diode behavior due to generation-recombination (GR) process in the depletion region was ruled out based on the fact that almost all reported data including ours show an n smaller than 2, and the current is not identical in both reverse and forward sides at lower voltages [16].

This work is licensed under a Creative Commons Attribution 4.0 License. For more information, see https://creativecommons.org/licenses/by/4.0/

TABLE 1. Growth conditions for i- and n-layers on (100)-oriented type IIb boron-doped diamond substrate.

	i-layer			n-layer	
	Stage 1	Stage 2	Stage 3	Stage 1	Stage 2
H_2 [sccm]	400	393	392	400	357
O_2 [sccm]	-	0.75	0.75	-	-
CH_4 [sccm]	-	-	7.0	-	3
TMP/H_2 [sccm]	-	-	-	-	40
Microwave power [W]	1100	1100	1100	1500	2500
Pressure [Torr]	60	60	60	65	75
Pyrometer [°C]	704	712	807	715	1025
Time [min]	5	5	240	5	10

Our study therefore focused on the possibility of barrier inhomogeneity in diamond Schottky diodes, which has been discussed by several groups [14], [17], [18], however lacks experimental confirmation. In this work, a diamond SPIND was fabricated and analyzed from room temperature up to 873 K. The presence of barrier height inhomogeneity was confirmed with experimental data.

II. EXPERIMENTAL DETAILS

N-type ($<10^{19}$ cm^{-3} phosphorus-doped) and intrinsic diamond layers were grown using CVD on the previously grown p-type ($\sim10^{20}$ cm^{-3} boron-doped) diamond on single crystalline substrates. The (100) boron-doped substrate (type IIb diamond) was purchased from the Technological Institute for Super-hard and Novel Carbon Materials, grown by high-pressure, high temperature (HPHT) technique with a boron-concentration of $\sim 1 \times 10^{20}$ cm^{-3}. The growth parameters for the intrinsic and phosphorus-doped diamond layers are detailed in Table 1.

For the fabrication of the diode structures, Al hard mask was patterned to etch down the diamond to the middle of the i-layer using a mixture of O_2/SF_6 plasma in an ICP/RIE system to achieve mesa isolation [19]. Partially mesa etch through the middle of the i-layer reduces the side wall leakage in contrast with the etch through the p-layer. After etching of the Al hard mask, samples were immersed in an acid mixture of H_2SO_4:HNO_3 3:1 at 220°C to oxygen terminate the surface and remove any surface conduction. The acid treatment improves adhesion of metal contacts. Ti/Pt/Au 50nm/50nm/150nm metal contacts were then deposited using an e-beam metal evaporator following by a lift-off process to pattern the contacts and annealing at 850°C, as shown in Fig. 1 (a). The n-side contact is on the top surface while for the p-side we used a backside contact taking the advantage of the conductive boron-doped substrate.

The I-V measurements were performed with Keithley 4200 (<0.1 A) and 2400 (<1 A) source/meters. One source/meter unit (SMU) was connected to the backside contact (p-type) to sweep the voltage and the other SMU was connected to the top side contact (n-type) as common. A high temperature stage (Linkam Scientific Instrument, Model T95-PE) was used to change the temperature from 298 K to 873 K. For the microscopic scale current measurement, an atomic force microscope (AFM) from Asylum Research (Model MFP3D) was used.

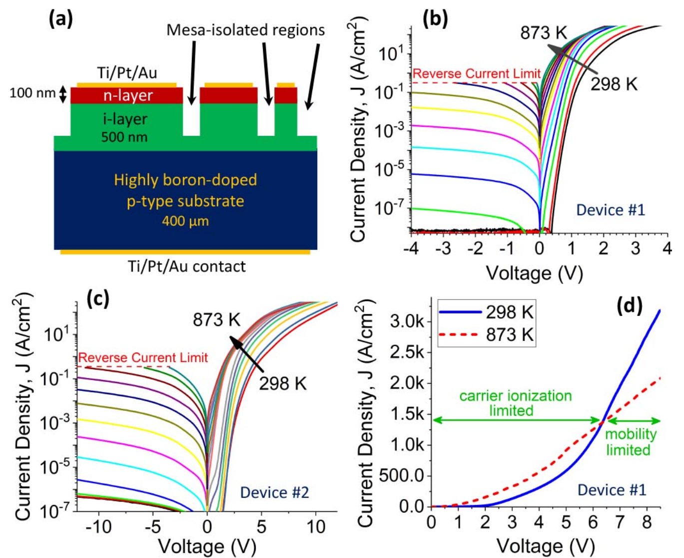

FIGURE 1. (a) Schematic view of the fabricated SPIND. The n-side contact is on the top surface and the p-contact is on the backside. (b) and (c) J-V characteristics as a function of temperature from 298-873 K for device #1 and #2, respectively. (d) Demonstration of the cross point between 298 and 873 K currents for device #1.

III. ELECTRICAL CHARACTERIZATION AND DISCUSSIONS

In Fig. 1 (b), the J-V characteristics of the SPIND (device #1) is shown in both forward and reverse directions from room temperature up to 873 K. The results show a rectification factor higher than 10^9 at room temperature, 1100 at 673 K, and $\sim$1 at 873 K. Increasing the n-layer doping slightly ($>10^{19}$ cm^{-3}) in another device (#2) resulted in a higher rectification factor ($\sim$20) but lower current at 873 K (Fig. 1 (c)), which shows that the SPIND can be easily modified for either high current or high rectification operations. As shown in Fig. 1 (d), device #1 offers a forward current density of about 3000 A/cm^2 at 8 V and shows a V^2 dependence indicative of injection mode transport, which follows the Mott-Gurney law in semiconductors [20]. The cross point between 298 K and 873 K currents above 6.5 V is a sign of mobility degradation due to the increased phonon scattering that overcomes the carrier ionization at high temperature [21], [22]. The rest of the analysis is dedicated to device #1.

Elevating the temperature resulted in an increase in the number of active dopants, thereby improving the forward conduction. Fig. 2 (a) shows the specific on-resistance ($R_{on.sp}$) at different temperatures as a function of voltage. The $R_{on.sp}$ decreased from 92 mΩ.cm^2 at 298 K to $\sim$5.7 mΩ.cm^2 at 873 K, at a bias of 1.5 V. However, at higher voltages the $R_{on.sp}$ increased slightly at higher temperatures compared to its room temperature value which is attributed to lower carrier mobility and increased substrate resistance (Fig. 2 (b)).

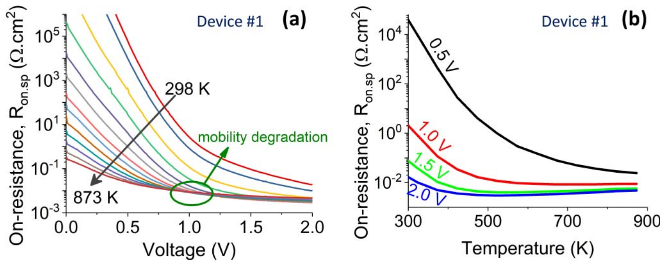

FIGURE 2. (a) Specific on-resistance ($R_{on.sp}$) vs forward voltage as a function of temperature from 298-873 K. (b) Specific on-resistance ($R_{on.sp}$) vs temperature at different voltages.

Since the main application of our SPIND is operating in high temperature environments like Venus atmosphere (~737 K), we have exposed all the diodes to high temperature up to 873 K for a long time to check the diode functionality and contacts stability. No degradation to diode performance has been observed after 10 cycles of temperatures from 298 K to 873 K.

To characterize the high temperature diode behavior, the conventional TE model (1) was used at first to extract n and zero-bias SBH (Φ_{B0}) at different temperatures [12].

$$I = AA^*T^2\exp\left(-\frac{q\varphi_{B0}}{k_BT}\right)\left[\frac{\exp(q(V-R_sI)}{nk_BT}-1\right] \quad (1)$$

where A is the geometric area, A^* is the Richardson's constant, T is the temperature, k_B is the Boltzmann constant, R_s is the series resistance, and V is the applied voltage. This model explains the conduction mechanism with an ideal homogeneous barrier over the entire geometric area of the Schottky contact. Theoretical A^* is equal to $\lambda_R(4\pi mk_B^2q/h^3)$, where λ_R is a material related constant, h is the Planck's constant, and m is the electron/hole mass [23]. Using the theoretical value of A^* for holes (=90 A/cm^2.K^2), n and Φ_{B0} were extracted at different temperatures from measured data to characterize thermionic emission of holes through the barrier (Fig. 3 (a)). n decreased with temperature (1.49 at 298K to 1.01 at 873K), and Φ_{B0} increased with temperature (1.11 eV at 298K to 1.51 eV at 873K). The deviations from an n of 1 and decrease in Φ_{B0} at lower temperatures indicated an inhomogeneous SBH over the contact area, as has been also reported in SiC [12], [13].

According to the inhomogeneity theory, at low temperatures, carriers without sufficient energy can only pass lower Schottky barriers, while at higher temperatures, more carriers gain sufficient energy to overcome higher barriers (covering larger area of the diode). This leads to the measurement of higher SBH at higher temperatures. In this case, per Tung's model, the behavior of the Schottky diode can be described with an effective SBH (Φ_{eff}). In order to extract Φ_{eff} and A^{**} a conventional Richardson's plot was used (Fig. 3 (b)). I_0 is the reverse saturation current and equals $AA^*T^2exp(-q\Phi_{B0}/k_BT)$. The value of the Φ_{eff} (= 0.92 eV) and A^{**} (=0.0461 A/cm^2.K^2) were found using the slope and y-axis intercept of the linear-fitted line, respectively.

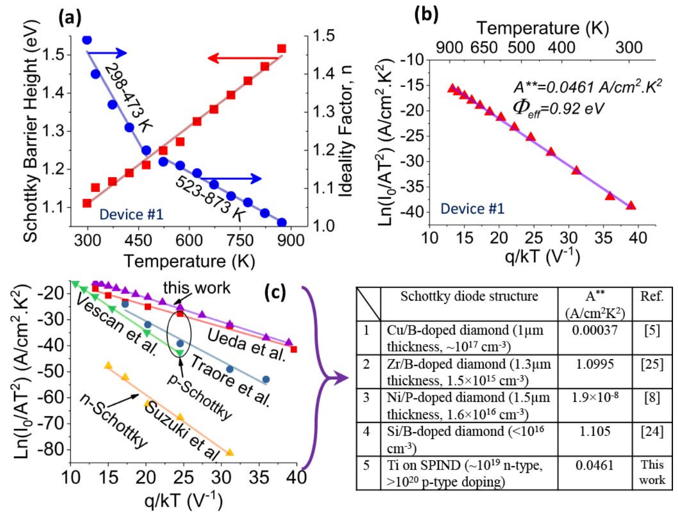

	Schottky diode structure	A^{**} (A/cm^{2}K^2)	Ref.
1	Cu/B-doped diamond (1µm thickness, ~10^{17} cm^{-3})	0.00037	[5]
2	Zr/B-doped diamond (1.3µm thickness, 1.5×10^{15} cm^{-3})	1.0995	[25]
3	Ni/P-doped diamond (1.5µm thickness, 1.6×10^{16} cm^{-3})	1.9×10^{-8}	[8]
4	Si/B-doped diamond (<10^{16} cm^{-3})	1.105	[24]
5	Ti on SPIND (~10^{19} n-type, >10^{20} p-type doping)	0.0461	This work

FIGURE 3. (a) Temperature dependence plot of the SBH and n for SPIND in the temperature range of 298-873 K. (b) Conventional Richardson's plot of $ln(I_0/AT^2)$ versus q/kT for SPIND. (c) Conventional Richardson's plot and A of other reported p- and n-type diamond Schottky diodes [5], [8], [24], [25].**

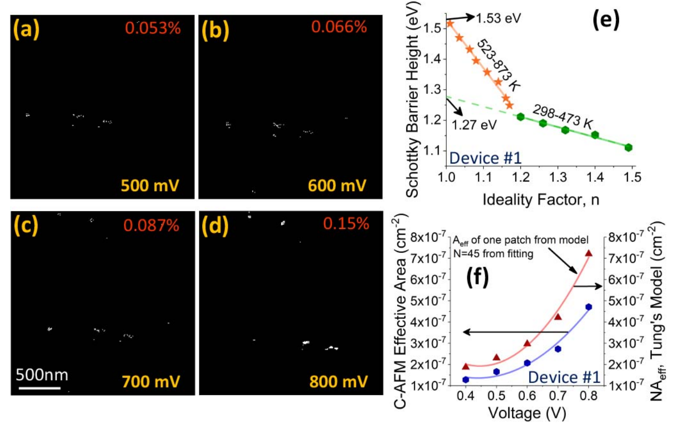

FIGURE 4. (a-d) Conductive-AFM current mapping of the Schottky diode at different forward bias voltages. The fraction of the active area is shown in top-right of the images. (e) Experimental SBH versus n plot for SPIND in the temperature range of 298-873 K. (f) Validation of Tung's model effective area using Conductive AFM current mapping. The A_{eff} was calculated from (3), then multiplied by N (= 45) to compare with C-AFM results.

The value of A^{**} is more than 3 orders of magnitude lower than the theoretical value (=90 A/cm^2.K^2) and along with deviations from ideality suggest that the conventional TE model cannot fully explain the diode behavior. A^{**} also was extracted from the high temperature data reported by other groups and summarized in Fig. 3 (c) [5], [8], [24], [25]. All these results show a much smaller A^{**} than in theory.

Conductive AFM was used to measure the local current flowing through the contact in the microscopic scale. As shown in Fig. 4 (a)-(d), the active area was a significantly smaller fraction of the contact surface area and changed with the applied voltage. It is worth noticing that, when the diameter of patches is comparable with depletion

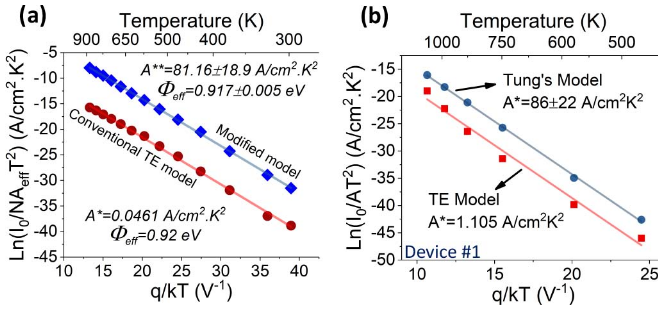

FIGURE 5. **(a) Modified Richardson's plot of $ln(I_0/N.A_{eff}.T^2)$ versus q/kT for SPIND in the temperature range of 298-873 K. The Richardson's plot using conventional TE model is also included for comparison. (b) Extraction of A** from high temperature data reported by Vescan et al. and comparison with extracted A** after applying Tung's model [24].**

width, the patches with smaller SBHs will be pinched-off by patches with larger SBHs, which makes the simple parallel model not accurate [16]. Therefore, A^{**} was determined by replacing the A with the actual effective area (NA_{eff}) in TE model (2).

$$I = NA_{eff}A^*T^2\exp\left(-\frac{q\Phi_{eff}}{k_BT}\right)\left[\frac{\exp(q(V-R_sI)}{nk_BT}-1\right] \quad (2)$$

where N is the number of active patches, and A_{eff} *is* the effective area of one patch, which can be calculated using (3).

$$A_{eff} = \frac{4\pi\gamma k_BT}{9q}\left(\frac{\eta}{V_{bb}}\right)^{2/3} \quad (3)$$

where V_{bb} is the band bending potential, η is equal to ε_s/qN_A, and γ is the patch parameter which is expressed as

$$\gamma = (\Phi_{B0}-\Phi_{eff})\left(\frac{\eta}{V_{bb}}\right)^{1/3} \quad (4)$$

The ideal case Φ_{B0} was extracted from Φ_{B0} vs n plot, by extrapolating the linear curve to the point where the n equals 1 (Fig. 4 (e)). The ideal Φ_{B0} was 1.27 eV for 298-473 K and 1.53 eV for 523-873 K range. η depends on carrier concentrations, which changes with temperature in diamond due to incomplete ionization at lower temperatures. This makes γ and A_{eff} dependent on the temperature as well. γ changes from 2.03×10^{-3} cm$^{2/3}$V$^{1/3}$ at 298 K to 1.9×10^{-4} cm$^{2/3}$V$^{1/3}$ at 873 K. A_{eff} varies between 2.3×10^{-9} and 1.96×10^{-12} cm^{-2} at different temperatures. Using the value of A_{eff} at different temperatures, the measurement data were fitted to (2) by changing N, A^*, R_s, and n. As shown in Fig. 4 (f), the total effective area from the model (NA_{eff}) at different bias voltages are in the same range as the values extracted from C-AFM results in room temperature. The offset can be due to the assumption of a constant N over the whole voltage range.

Using modified Richardson's plot, where area constant was replaced by whole effective area (Fig. 5 (a)), the A^{**} was extracted to be 81.16±18.9 A/cm^2.K^2, which is much closer to theoretical value. This modified model also was applied to the work done by Vescan *et al.* (Fig. 5 (b)), which resulted in resolving the Richardson's constant discrepancy from their data as well and showed that Tung's model is also applicable for diamond p-Schottky diodes.

IV. CONCLUSION

This work highlights the high temperature operation of diamond diodes (up to 873K). The results were analyzed to explain the physical reason behind extracting a lower Richardson's constant compared to the theoretical value. The discrepancy was explained using Tung's barrier inhomogeneity model yielding $A^{**} = 81.16 \pm 8.9$ A/cm^2.K^2. Conductive AFM studies further validated the use of the barrier inhomogeneity model.

ACKNOWLEDGMENT

The authors gratefully acknowledge Prof. S. M. Goodnick for valuable discussions and providing the high temperature stage for measurements.

REFERENCES

[1] H. Umezawa, K. Ikeda, R. Kumaresan, N. Tatsumi, and S.-I. Shikata, "Increase in reverse operation limit by barrier height control of diamond schottky barrier diode," *IEEE Electron Device Lett.*, vol. 30, no. 9, pp. 960–962, Sep. 2009, doi: 10.1109/LED.2009.2026439.

[2] H. Umezawa, M. Nagase, Y. Kato, and S.-I. Shikata, "High temperature application of diamond power device," *Diamond Rel. Mater.*, vol. 24, pp. 201–205, Apr. 2012, doi: 10.1016/j.diamond.2012.01.011.

[3] H. Umezawa *et al.*, "Leakage current analysis of diamond Schottky barrier diode," *Appl. Phys. Lett.*, vol. 90, no. 7, pp. 1–4, 2007, doi: 10.1063/1.2643374.

[4] D. J. Twitchen *et al.*, "High-voltage single-crystal diamond diodes," *IEEE Trans. Electron Devices*, vol. 51, no. 5, pp. 826–828, May 2004, doi: 10.1109/TED.2004.826867.

[5] K. Ueda, K. Kawamoto, and H. Asano, "High-temperature and high-voltage characteristics of Cu/diamond Schottky diodes," *Diamond Rel. Mater.*, vol. 57, pp. 28–31, Aug. 2015, doi: 10.1016/j.diamond.2015.03.006.

[6] R. Hathwar, M. Dutta, F. A. M. Koeck, R. J. Nemanich, S. Chowdhury, and S. M. Goodnick, "Temperature dependent simulation of diamond depleted Schottky PIN diodes," *J. Appl. Phys.*, vol. 119, no. 22, 2016, Art. no. 225703, doi: 10.1063/1.4953385.

[7] T. Makino *et al.*, "Diamond Schottky p-n diode with high forward current density," *Phys. Status Solidi Appl. Mater. Sci.*, vol. 206, no. 9, pp. 2086–2090, 2009, doi: 10.1002/pssa.200982228.

[8] M. Suzuki *et al.*, "Electrical characteristics of n-type diamond Schottky diodes and metal/diamond interfaces," *Phys. Status Solidi Appl. Mater. Sci.*, vol. 203, no. 12, pp. 3128–3135, 2006, doi: 10.1002/pssa.200671124.

[9] T. Makino *et al.*, "Diamond Schottky-*pn* diode with high forward current density and fast switching operation," *Appl. Phys. Lett.*, vol. 94, no. 26, pp. 2007–2010, 2009, doi: 10.1063/1.3159837.

[10] M. Dutta, F. A. M. Koeck, R. Hathwar, S. M. Goodnick, R. J. Nemanich, and S. Chowdhury, "Demonstration of diamond-based Schottky p-i-n diode with blocking voltage > 500 v," *IEEE Electron Device Lett.*, vol. 37, no. 9, pp. 1170–1173, Sep. 2016, doi: 10.1109/LED.2016.2592500.

[11] J. H. Werner and H. H. Güttler, "Barrier inhomogeneities at Schottky contacts," *J. Appl. Phys.*, vol. 69, no. 3, pp. 1522–1533, 1991, doi: 10.1063/1.347243.

[12] A. F. Hamida, Z. Ouennoughi, A. Sellai, R. Weiss, and H. Ryssel, "Barrier inhomogeneities of tungsten Schottky diodes on 4H-SiC," *Semicond. Sci. Technol.*, vol. 23, no. 4, 2008, Art. no. 045005, doi: 10.1088/0268-1242/23/4/045005.

[13] F. Roccaforte, F. L. Via, V. Raineri, R. Pierobon, and E. Zanoni, "Richardson's constant in inhomogeneous silicon carbide Schottky contacts," *J. Appl. Phys.*, vol. 93, no. 11, pp. 9137–9144, 2003, doi: 10.1063/1.1573750.

[14] A. Fiori, T. Teraji, and Y. Koide, "Schottky-barrier inhomogeneities in WC/p-diamond at high temperature," in *Proc. Int. Conf. Solid State Devices Mater.*, 2017, pp. 380–381, doi: 10.7567/ssdm.2014.ps-14-10.
[15] F. Iucolano, F. Roccaforte, F. Giannazzo, and V. Raineri, "Barrier inhomogeneity and electrical properties of Pt/GaN Schottky contacts," *J. Appl. Phys.*, vol. 102, no. 11, 2007, Art. no. 113701, doi: 10.1063/1.2817647.
[16] R. T. Tung, "Electron transport at metal-semiconductor interfaces: General theory," *Phys. Rev. B, Condens. Matter*, vol. 45, no. 23, pp. 13509–13523, 1992, doi: 10.1103/PhysRevB.45.13509.
[17] M. Craciun, C. Saby, P. Muret, and A. Deneuville, "A 3.4 eV potential barrier height in Schottky diodes on boron-doped diamond thin films," *Diamond Rel. Mater.*, vol. 13, no. 2, pp. 292–295, 2004, doi: 10.1016/j.diamond.2003.10.012.
[18] A. Traoré, *High Power Diamond Schottky Diode*, Université de Grenoble, Grenoble, France, 2015.
[19] M. Dutta, F. A. M. Koeck, W. Li, R. J. Nemanich, and S. Chowdhury, "High voltage diodes in diamond using (100)- and (111)-substrates," *IEEE Electron Device Lett.*, vol. 38, no. 5, pp. 600–603, May 2017, doi: 10.1109/LED.2017.2681058.
[20] N. F. Mott and R. W. Gurney, *Electronic Processes in Ionic Crystals*. New York, NY, USA: Oxford Univ. Press, 1940.
[21] M. Gabrysch, *Charge Transport in Single-Crystalline CVD Diamond*, Acta Universitatis Upsaliensis, Uppsala, Sweden, 2010.
[22] H. Pernegger *et al.*, "Charge-carrier properties in synthetic single-crystal diamond measured with the transient-current technique," *J. Appl. Phys.*, vol. 97, no. 7, pp. 1–9, 2005, doi: 10.1063/1.1863417.
[23] C. R. Crowell, "The Richardson constant for thermionic emission in Schottky barrier diodes," *Solid-State Electron.*, vol. 8, no. 4, pp. 395–399, 1965, doi: 10.1016/0038-1101(65)90116-4.
[24] A. Vescan, I. Daumiller, P. Gluche, W. Ebert, and E. Kohn, "Very high temperature operation of diamond Schottky diode," *IEEE Electron Device Lett.*, vol. 18, no. 11, pp. 556–558, Nov. 1997, doi: 10.1109/55.641444.
[25] A. Traoré, P. Muret, A. Fiori, D. Eon, E. Gheeraert, and J. Pernot, "Zr/oxidized diamond interface for high power Schottky diodes," *Appl. Phys. Lett.*, vol. 104, no. 5, 2014, Art. no. 052105, doi: 10.1063/1.4864060.